PAPER

Dynamics at the threshold for blowup for supercritical wave equations outside a ball*

IOP Publishing | London Mathematical Society Nonlinearity

Nonlinearity **33** (2020) 3195–3205 https://doi.org/10.1088/1361-6544/ab8352

Dynamics at the threshold for blowup for supercritical wave equations outside a ball*

Piotr Bizoń[1] **and Maciej Maliborski**[2,3]

[1] Institute of Theoretical Physics, Jagiellonian University, Kraków, Poland
[2] Gravitational Physics, Faculty of Physics, University of Vienna, Boltzmanngasse 5, A-1090 Vienna, Austria

E-mail: bizon@th.if.uj.edu.pl and maciej.maliborski@univie.ac.at

Received 5 September 2019, revised 22 March 2020
Accepted for publication 25 March 2020
Published 26 May 2020

Abstract

We consider spherically symmetric supercritical focusing wave equations outside a ball. Using mixed analytical and numerical methods, we show that the threshold for blowup is given by a codimension-one stable manifold of the unique static solution with exactly one unstable direction. We analyse in detail the convergence to this critical solution for initial data fine-tuned to the threshold.

Keywords: nonlinear wave equations, threshold for blowup, quasinormal modes
Mathematics Subject Classification numbers: 35L71, 35L20, 35P99.

(Some figures may appear in colour only in the online journal)

1. Introduction

This paper is concerned with the focusing semilinear wave equation for a real scalar field $\phi(t, x)$,

$$\phi_{tt} = \Delta\phi + \phi^{2p+1}, \tag{1}$$

outside a unit ball in $\mathbb{R}^d$ for odd $d \geqslant 3$. Here p is a positive integer greater than $\frac{2}{d-2}$ which corresponds to the supercitical regime. We restrict ourselves to spherically symmetric solutions

*This research was supported by the Polish National Science Centre Grant No. 2017/26/A/ST2/00530. Computations have been performed on Minerva cluster of the Max-Planck Institute for Gravitational Physics.

[3]Author to whom any correspondence should be addressed.

$\phi(t, r)$, where $r = |x|$, satisfying the Dirichlet boundary condition $\phi(t, 1) = 0$, hence we solve

$$\phi_{tt} = \phi_{rr} + \frac{d-1}{r}\phi_r + \phi^{2p+1} \quad \text{for } r \geqslant 1 \quad \text{with } \phi(t, 1) = 0. \tag{2}$$

Initial data $(\phi(0, r), \phi_t(0, r))$ are assumed to be smooth, exponentially localized, and compatible with the boundary condition.

Let us first briefly recall what is known about solutions of equation (2) in the whole space. For small initial data the solutions are global in time and scatter to zero for $t \to \infty$ [1]. The behaviour of large solutions is only partially understood. In the case $d = 3$, the numerical studies reported in [2] show that for generic large initial data the solutions blow up as $\phi \sim (T - t)^{-1/p}$ for $t \nearrow T < \infty$. The nonlinear stability of this ODE blowup was proved by Donninger and Schörkhuber [3]. In addition, there exists a countable family of unstable self-similar solutions which correspond to non-generic finite time blowups [4] and the unique self-similar solution with exactly one unstable direction was shown numerically to be critical in the sense that its codimension-one stable manifold separates dispersive and singular solutions [2]. Recently, the analogous critical dynamics at the threshold for blowup has been analysed for the cubic wave equation in higher dimensions [5]; remarkably, for $d \geqslant 5$ the critical self-similar solution has been found explicitly which allowed the authors to prove rigorously its codimension-one stability [6].

The presence of the obstacle does not affect the qualitative behaviour of generic solutions, that is small solutions scatter to zero, while large solutions exhibit the ODE blowup. However, the obstacle breaks the scaling symmetry thereby excluding self-similar solutions and at the same time allowing for nontrivial static solutions. These static solutions are known from studies of elliptic equations [7, 8] but, as far as we know, their role in dynamics has not been studied [note added in proof: after completion of this paper, there appeared a preprint by Duyckaerts and Yang [9] in which they proved that any global-in-time solution of equation (2) either scatters to zero or converges (up to a dispersive term) to one of the nonzero static solutions; the proof is based on the concentration-compactness technique which gives no information about the rate of convergence]. For completeness, in the next section we give an elementary proof of existence of a countable family of static solutions with increasing number of nodes. We also prove that the nodal index of these solutions counts the number of their unstable modes. The main goal of this paper is to show, using mixed numerical and analytical methods, that the static solution with one unstable mode plays the role a critical solution whose codimension-one stable manifold separates dispersive and singular solutions.

2. Static solutions and their stability

For time-independent solutions equation (2) reduces to the radial Lane–Emden equation

$$\phi_{rr} + \frac{d-1}{r}\,\phi_r + \phi^{2p+1} = 0, \tag{3}$$

which after the change of variables (introduced by Fowler in [10])

$$s = \ln r, \quad h(s) = r^{1/p}\phi(r) \tag{4}$$

transforms into the autonomous ordinary differential equation ($\cdot = \mathrm{d}/\mathrm{d}s$)

$$\ddot{h} + \left(d - 2 - \frac{2}{p}\right)\dot{h} - \frac{1}{p}\left(d - 2 - \frac{1}{p}\right)h + h^{2p+1} = 0. \tag{5}$$

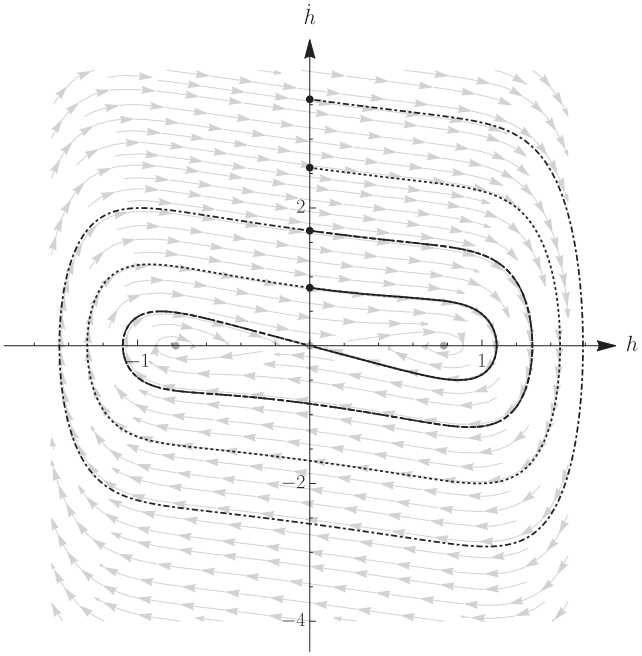

Figure 1. Phase portrait $(h, \dot{h})$ for a sample pair $(d, p) = (3, 3)$. The trajectories of the first four nonzero static solutions h_n are plotted with distinct line styles and their starting points $(h_n(0), \dot{h}_n(0)) = (0, b_n)$ are marked with black circles.

Table 1. Parameters b_n and c_n of the first three nonzero static solutions for a few pairs (d, p).

(d, p)	(b_1, c_1)	(b_2, c_2)	(b_3, c_3)
(3, 3)	(0.84261, −4.46847)	(1.67035, 21.7658)	(2.58523, −62.5081)
(3, 4)	(1.20653, −3.71646)	(2.48958, 13.0365)	(3.90145, −28.9009)
(3, 5)	(1.41849, −3.35818)	(2.95061, 10.1979)	(4.61581, −20.3151)
(5, 1)	(5.51059, −22.5426)	(12.4733, 209.872)	(21.5494, −1005.52)
(5, 2)	(7.70805, −8.22701)	(18.1434, 32.8788)	(30.9438, −79.2027)
(5, 3)	(7.69629, −5.64440)	(17.4958, 17.8598)	(28.8616, −36.3276)

For $p > \frac{2}{d-2}$ the 'friction' coefficient in (5) is positive and from an elementary phase-plane analysis (see the phase portrait in figure 1) it follows that there exist infinitely many initial values $(h_n(0), \dot{h}_n(0)) = (0, b_n)$, where n is a positive integer, for which the phase trajectory makes n half rotations around the origin and then tends to the saddle point at the origin along the stable direction

$$h_n(s) \sim c_n \, \mathrm{e}^{-(d-2-1/p)s} \quad \text{for } s \to \infty. \tag{6}$$

In terms of the original variables these trajectories correspond to finite energy static solutions $\phi_n(r)$ which vanish at $r = 1$ and decay as c_n/r^{d-2} for $r \to \infty$. The first few values of parameters b_n and c_n determined numerically for several pairs (d, p) are given in table 1.

We remark that no static solutions exist in the critical and subcritical cases $p \leqslant 2/(d-2)$, as follows, for instance, from the identity

$$\frac{1}{2}\dot{h}^2(0) = \left(d - 2 - \frac{2}{p}\right)\int_0^\infty \dot{h}^2(s)\,\mathrm{d}s, \tag{7}$$

which arises from multiplying equation (5) by $\dot{h}$ and integrating by parts.

The role of static solutions in dynamics depends on their stability properties. To determine the linear stability of the solution $\phi_n(r)$, we substitute $\phi(t,r) = \phi_n(r) + w(t,r)$ into (2). Dropping nonlinear terms in w, we get the linearized equation

$$w_{tt} = w_{rr} + \frac{d-1}{r}w_r + (2p+1)\phi_n^{2p}w. \tag{8}$$

Substituting $w(t,r) = \mathrm{e}^{\lambda t}v(r)$, we obtain the eigenvalue problem

$$L_n v := \left(-\frac{\mathrm{d}^2}{\mathrm{d}r^2} - \frac{d-1}{r}\frac{\mathrm{d}}{\mathrm{d}r} - (2p+1)\phi_n^{2p}(r)\right)v = -\lambda^2 v. \tag{9}$$

For each n the operator L_n, acting on L^2-functions that vanish at $r=1$, is essentially self-adjoint. Since $\phi_n(r)$ is bounded and decays to zero at infinity, L_n has a continuous spectrum $[0,\infty)$. Note that the function generated by scaling

$$v_0^{(n)}(r) = \frac{\mathrm{d}}{\mathrm{d}\alpha}\alpha^{1/p}\phi_n(\alpha r)\bigg|_{\alpha=1} = r\phi_n'(r) + \frac{1}{p}\phi_n(r) \tag{10}$$

solves equation (9) for $\lambda = 0$ (but it is not an eigenfunction because it does not vanish at $r=1$). From the phase-plane analysis above it follows that $v_0^{(n)}(r)$ has exactly n zeros which implies by the Sturm oscillation argument that the operator L_n has exactly n negative eigenvalues, hereafter denoted by $-(\lambda_k^{(n)})^2$ $(k=1,\ldots,n)$. Consequently, the static solution ϕ_n has exactly n unstable modes $v_k^{(n)}(r)\mathrm{e}^{\lambda_k^{(n)}t}$. In what follows we focus on dynamics near the static solution $\phi_1(r)$ which has exactly one unstable mode $v_1(r)\mathrm{e}^{\lambda_1 t}$ (henceforth we drop the superscript (n) on the eigenvalues and eigenfunctions). Due to the presence of the unstable mode, generic solutions of the linearized equation (8) grow exponentially. This instability can be eliminated by preparing initial data belonging to the codimension-one stable subspace. For such special initial data the solutions decay in time due to a combination of two dispersive effects: the quasinormal ringdown and the polynomial tail. For exponentially localized initial data the rate of decay of the tail is determined by the fall-off of the potential term in (8), namely if the potential falls off as $r^{-\gamma}$ for $r\to\infty$, then $w(t,r)\sim t^{-\gamma-\frac{1}{2}(d-3)}$ for any fixed $r>1$ and $t\to\infty$ (see [11] for $d=3$ and equation (26) in [12] for odd $d\geqslant 5$). In the case at hand, $\phi_1(r)$ decays as $r^{-(d-2)}$, hence $\gamma = 2p(d-2)$. The ringdown is determined by the quasinormal modes which are solutions of the eigenvalue equation (9) with $\mathrm{Re}(\lambda) < 0$ satisfying the outgoing wave condition $v(r)\sim \mathrm{e}^{-\lambda r}$ for $r\to\infty$. As the concept of quasinormal modes is inherently related to the loss of energy by radiation, the unitary evolution (8) and the associated self-adjoint eigenvalue problem (9) do not provide a natural setting for analysing quasinormal modes, both from the conceptual and computational viewpoints. For this reason we postpone the discussion of quasinormal modes until the next section where a new nonunitary formulation will be introduced.

3. Characteristic initial-boundary value formulation

The rest of the paper is devoted to dynamics of convergence to ϕ_1 for initial data fine-tuned to the threshold. To this order we introduce the null coordinate $u = t - r$ and the inverse radial coordinate $x = 1/r$ which compactifies the spatial domain to the interval $0 \leqslant x \leqslant 1$. Then $f(u,x) = r^{\frac{d-1}{2}}\phi(t,r)$ satisfies the equation

$$2f_{ux} + x^2 f_{xx} + 2xf_x - \frac{1}{4}(d-3)(d-1)f + x^\alpha f^{2p+1} = 0, \quad f(u,1) = 0, \tag{11}$$

where $\alpha = \frac{1}{2}p(d-1) - 1$. We note in passing that equation (11) can be written as the conservation law

$$\partial_x\left(f_u^2 + x^2 f_u f_x\right) = \partial_u\left(\frac{1}{2}x^2 f_x^2 + \frac{1}{8}(d-3)(d-1)f^2 - \frac{1}{2p+2}x^\alpha f^{2p+2}\right), \tag{12}$$

which upon integration gives the energy loss formula

$$\frac{\mathrm{d}E}{\mathrm{d}u} = -f_u(u,0)^2, \tag{13}$$

where

$$E[f] = \int_0^1 \left(\frac{1}{2}x^2 f_x^2 + \frac{1}{8}(d-3)(d-1)f^2 - \frac{1}{2p+2}x^\alpha f^{2p+2}\right)\mathrm{d}x. \tag{14}$$

As follows from section 2, equation (11) has infinitely many static solutions $f_n(x)$ which behave as $f_n(x) \sim c_n x^{\frac{d-3}{2}}$ near $x = 0$ and vanish at $x = 1$. These static solutions are critical points of the energy functional $E[f]$.

We now repeat the linear stability from the previous section by substituting $f(u,x) = f_1(x) + \mathrm{e}^{\lambda u}v(x)$ into (11) and linearizing. This yields the eigenvalue problem

$$x^2 v'' + 2xv' + 2\lambda v' - \frac{1}{4}(d-3)(d-1)v + (2p+1)x^\alpha f_1^{2p}(x)v = 0, \quad v(1) = 0. \tag{15}$$

An advantage of this formulation is that it allows us to treat quasinormal modes as genuine eigenfunctions of the generators of time translations of the null foliation; see [13] for the discussion of a model problem of the form (15). To do so we must specify the desired behaviour of eigenfunctions at $x = 0$ which is rather subtle because this endpoint is an essential singularity. The two linearly independent solutions of equation (15) near $x = 0$ have the following leading behaviours

$$v_g(x) \sim 1, \quad v_b(x) \sim \mathrm{e}^{2\lambda/x}, \tag{16}$$

where the subscripts g and b stand for 'good' and 'bad' solutions, respectively. At $x = 0$ the solution $v_g(x)$ admits a formal Taylor series, while the solution $v_b(x)$ has an essential singularity. In terms of the original variables, these two solutions correspond to the outgoing and ingoing waves, respectively, thus we demand that the eigenfunctions have no admixture of v_b. Having a good solution near $x = 0$, one can shoot it towards $x = 1$ and determine the eigenvalues from the boundary condition $v(1) = 0$. Since the formal Taylor series of v_g is in general

divergent, in practice we take the asymptotic expansion of $v_g(x)$ at some small x_0 and truncate it at the least term. While this optimal truncation approach works very well in the case of positive (unstable) eigenvalues, it is not precise enough for the eigenvalues with $\mathrm{Re}(\lambda) < 0$ because in this case the bad solution $v_b(x)$ is smaller than any power of x for $x \to 0^+$. To capture such a small term we use the Borel summation method which goes as follows. Given a formal power series $v_g(x) = \sum_{k=0}^{\infty} a_k x^k$, we Borel transform it

$$\mathcal{B}(x) = \sum_{k=0}^{\infty} \frac{a_k}{k!} x^k. \tag{17}$$

and then take the Laplace transform to get the Borel sum

$$\mathcal{B}_S(x) = \int_0^{+\infty} \mathrm{e}^{-t}\, \mathcal{B}(tx)\, \mathrm{d}t. \tag{18}$$

In practice, we truncate the series in (17) at some high order $2K$ and accelerate the convergence by using the (diagonal) Padé approximation $P_K\mathcal{B}$. Because of possible poles of the Padé approximation on the real axis, we deform the integration contour in (18) by introducing the following path on the complex plane $\gamma(\varepsilon) = \gamma_1 \cup \gamma_2$ with

$$\gamma_1 : [0, \varepsilon] \ni s \to is \in \mathbb{C}, \quad \gamma_2 : [0, \infty) \ni s \to i\varepsilon + s \in \mathbb{C}, \tag{19}$$

where ε is a free real parameter[4] (since the integrand decays sufficiently fast we need not to close the contour 'at infinity'). In our calculations we took the mean of integrals along the contours $\gamma(\varepsilon)$ and $\gamma(-\varepsilon)$, thus we approximated (18) by

$$\mathcal{B}_S(x) \approx \frac{1}{2}\int_{\gamma(\varepsilon)} \mathrm{e}^{-t}\, P_K\mathcal{B}(tx)\, \mathrm{d}t + \frac{1}{2}\int_{\gamma(-\varepsilon)} \mathrm{e}^{-t}\, P_K\mathcal{B}(tx)\mathrm{d}r. \tag{20}$$

and then computed these integrals numerically.

Having set up initial conditions at x_0 (either by the optimal truncation or Borel summation), we integrated equation (15) using an adaptive Runge–Kutta method of 8th order and then determined the eigenvalues by solving the boundary condition $v(1) = 0$ with Newton's method (see table 2). To suppress round-off errors we used an extended precision arithmetics, typically with more than 20 digits. Particularly demanding was the computation of the first stable eigenvalue λ_2 for $d = 3$. For example, in the case $(d, p) = (3, 3)$ we used $x_0 \approx 0.008\,25$, $K = 128$, $\varepsilon = 10$ and Gauss quadratures with 38 and 128 nodes for Gauss–Legendre and Gauss–Laguerre rules to compute the integrals (20) along γ_1 and γ_2, respectively. This scheme provided an accurate enough initial conditions for the shooting algorithm to produce $\lambda_2 \approx -0.043\,283\,58\ldots$ whose first 15 digits did not depend on the choice of the starting point x_0 which made us feel confident that the result is correct.

In the appendix A we describe a different method of finding the spectrum of the linearized problem which reproduces all the above eigenvalues except for those that lie on the negative real axis.

[4] In practice, having an initial guess for the eigenvalue λ (based on the optimal truncation method), we looked at the distribution of poles of $P_K\mathcal{B}(z)$ on the complex z-plane to estimate the value of the parameter ε. In most cases $\varepsilon = 1$ worked reasonably well.

Table 2. The unstable eigenvalue λ_1 and two least damped stable eigenvalues λ_2, λ_3 of the linearized operator around the static solution f_1 for several pairs (d,p). All given digits are significant.

(d,p)	λ_1	λ_2	λ_3
(3, 3)	0.437 6132	−0.043 283 58	$-0.735\,9469 \pm 0.661\,1351i$
(3, 4)	0.911 9156	−0.125 663 11	$-0.911\,2554 \pm 1.228\,442i$
(3, 5)	1.393 964	−0.215 784 21	$-0.958\,9717 \pm 1.608\,909i$
(5, 1)	1.412 962	$-0.158\,0264 \pm 0.209\,4073i$	$-3.663\,357 \pm 1.863\,078i$
(5, 2)	4.006 646	$-0.594\,3277 \pm 0.478\,9266i$	$-5.062\,170 \pm 5.850\,155i$
(5, 3)	6.472 988	$-0.945\,0331 \pm 0.503\,2462i$	$-5.050\,332 \pm 8.049\,461i$

4. Critical evolution

In this section we give numerical evidence supporting our conjecture that the static solution f_1 sits at the threshold for generic blowup.

Before presenting results we briefly describe our method of solving numerically the initial-boundary value problem (11). We use the method of lines with a spectral element method [15] for space discretization. The starting point of this approach is a weak formulation of equation (11). The spatial domain is divided into non-overlapping intervals and on each interval the integral is approximated using the Gauss–Legendre quadrature formula. We typically use 16 grid points in each of 9 equal size intervals of the spatial domain. The coupling between the intervals is enforced by the requirement of smoothness. At the sphere $x = 1$ we impose the Dirichlet condition, while at null infinity $x = 0$ no condition is imposed. The resulting equations are integrated in time using the 6th order Runge–Kutta scheme with a fixed time step. The presence of the mixed derivative in equation (11) required a solution of the algebraic system at the internal steps of the Runge–Kutta scheme.

To get a clear picture of near critical evolution it was instrumental to use high precision arithmetics which is computationally expensive. The numerical algorithm described above gave satisfactory results at an acceptable cost. The efficiency of the spectral element method is due to its fast convergence and the sparse (block diagonal) structure of matrices. To further speed up calculations we use a parallel version of the bisection search to fine tune the initial data. The code was written in Mathematica.

We illustrate our numerical results for a one-parameter family of initial data

$$f(0,x) = a \sin^2(\pi x)\, \mathrm{e}^{-200(x-1/2)^2}. \tag{21}$$

which interpolates between dispersion to zero for small amplitudes a and the ODE blowup for large a. Using bisection we fine tune the amplitude to the critical value a_* separating these two generic behaviours. For such fine-tuned initial data we observe for intermediate times the convergence to the static solution f_1. This is shown in figure 2 for two pairs $(d,p) = (3,3)$ and $(5,2)$.

For intermediate times, when the nearly critical solution is close to f_1, the dynamics is well approximated (for any fixed x) by the formula

$$f(u,x) = f_1(x) + c_1\, \mathrm{e}^{\lambda_1 u} + \underbrace{\mathrm{Re}\left(c_2\, \mathrm{e}^{\lambda_2 u}\right) + \ldots}_{\text{ringdown}} + \underbrace{c_3 u^{-\beta}\left(1 + \frac{c_4}{u} + \frac{c_5}{u^2} + \ldots\right)}_{\text{tail}}, \tag{22}$$

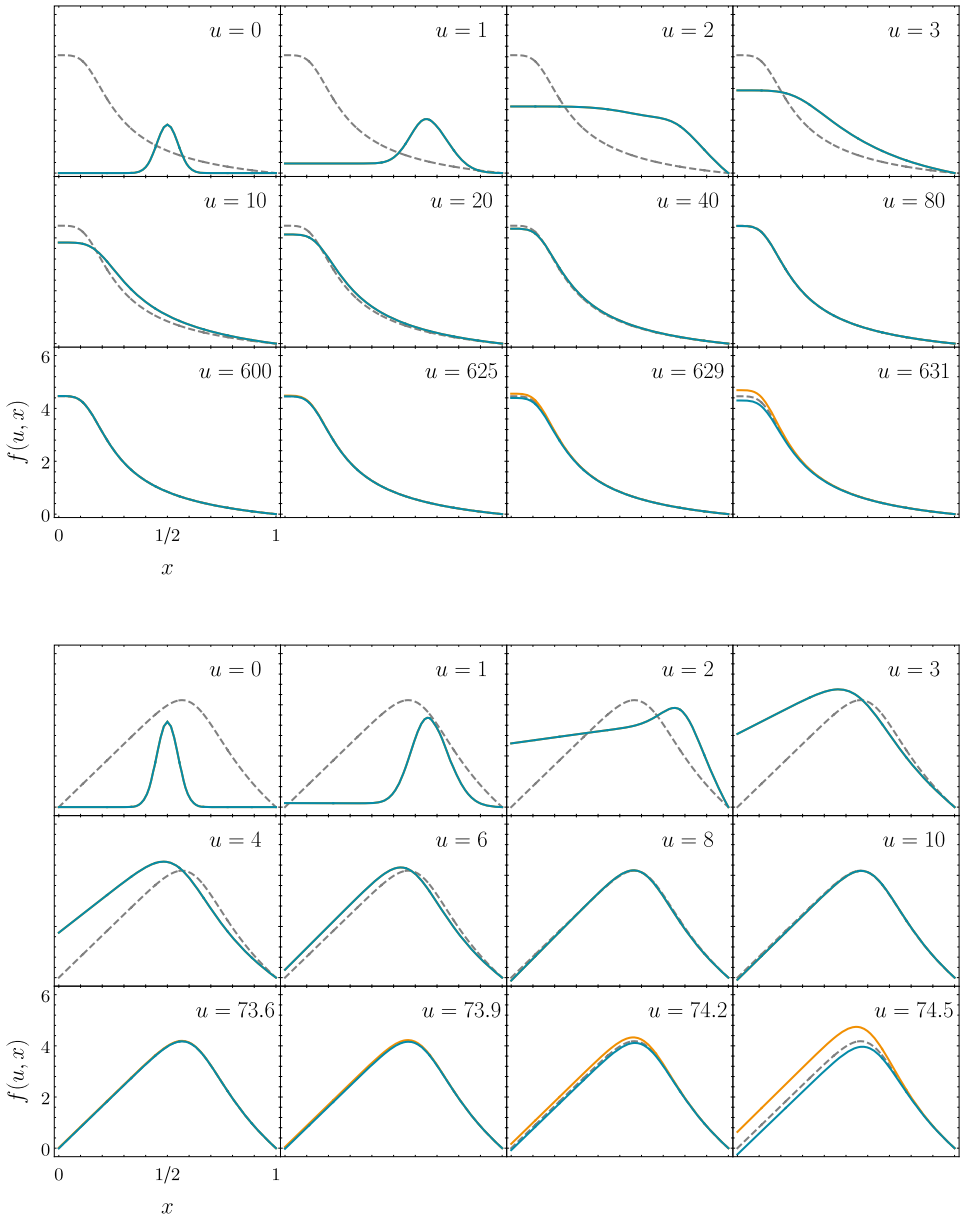

Figure 2. Snapshots of near critical evolution of initial data (21) for $(d, p) = (3, 3)$ where $a_* \approx 1.834\,21$ (upper plot) and $(d, p) = (5, 2)$ where $a_* \approx 0.338\,53$ (lower plot). The amplitudes of marginally subcritical (blue lines) and supercritical (orange lines) data differ by 10^{-128}. Initially the solutions evolve together, approach f_1 (dashed lines) for intermediate times, and eventually depart in opposite directions.

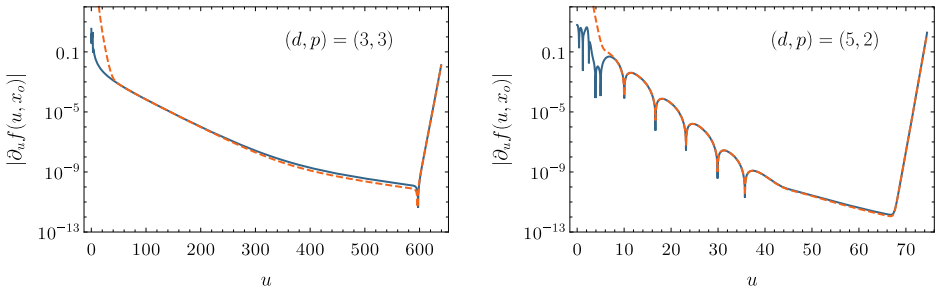

Figure 3. Pointwise convergence to f_1 at a sample interior point $x_o = 5/9$ for the same marginally subcritical data as in figure 2. The dashed lines depict the fits based on formula (22). For $(d,p) = (5,2)$ the evolution has two well-separated phases: the quasinormal ringdown followed by the polynomial tail. For $(d,p) = (3,3)$ the least damped quasinormal mode is non-oscillatory and very slowly decaying which makes it harder to separate it from the tail.

where c_i are (x dependent) parameters and dots denote subleading terms. For exactly critical data the coefficient c_1 vanishes. Our bisection procedure ensures that $c_1 \sim a - a_*$ is very small, typically of order 10^{-128}, which gives a reasonably long span of time $\propto -\frac{1}{\lambda_1}\log|a-a_*|$ over which the approximation (22) is expected to hold and can be fitted to the nearly critical solution shown in figure 2. Performing this fit we reproduce the eigenvalues λ_1 and λ_2 with precision of 0.01% which is very reassuring; see figure 3. For the tail, we fix the exponent $\beta = p(d-1) + \frac{1}{2}(d-3)$, according to formula (11) in [14] for the nonlinear tail.

Appendix A. Pseudospectral solution of the linear problem

Here we present a simple algebraic method of solving the linearized characteristic initial-boundary value problem which reproduces most (but not all) results from section 3.

Linearization of equation (11) around a static solution f_n yields

$$\partial^2_{ux} v = L_n v, \tag{23}$$

with

$$L_n := \frac{1}{2}\left(-x^2\partial_x^2 - 2x\partial_x + \frac{1}{4}(d-3)(d-1) - (2p+1)x^\alpha f_n^{2p}(x)\right). \tag{24}$$

Discretization in space transforms equation (23) into a system of N coupled constant-coefficient ODEs, where N is the number of degrees of freedom introduced by discretization. In the case at hand, N is the number of Chebyshev polynomials used in the spatial approximation of $v(u,x)$. This semi-discrete problem has the form

$$\mathbf{D}\frac{\mathrm{d}}{\mathrm{d}u}\mathbf{v} = \mathbf{L}_n\mathbf{v}, \tag{25}$$

where $\mathbf{v}$ is a vector of unknowns, $\mathbf{D}$ is an invertible discrete version of ∂_x which incorporates the boundary condition $v(u,1) = 0$, and $\mathbf{L}_n$ is a discretization of L_n. We rewrite (25) as

$$\frac{\mathrm{d}}{\mathrm{d}u}\mathbf{v} = \mathbf{D}^{-1}\mathbf{L}_n\mathbf{v}, \tag{26}$$

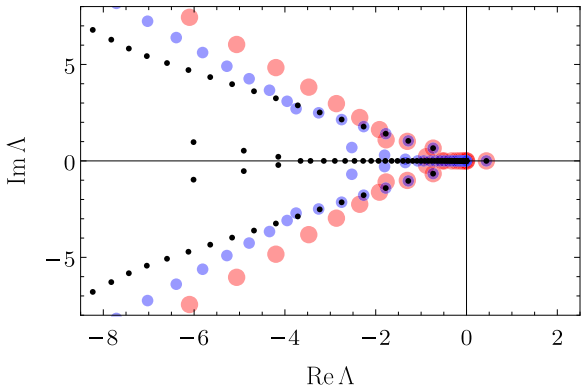

Figure A1. Eigenvalues Λ_i of the discrete operator $\mathbf{D}^{-1}\mathbf{L}_0$ in the $(d,p)=(3,3)$ case for different numbers of Chebyshev polynomials used in the approximation: $N=64$ (red), $N=128$ (blue), $N=256$ (black). As N increases, we observe accumulation of spurious eigenvalues on the negative real axis and convergence to the genuine eigenvalues elsewhere.

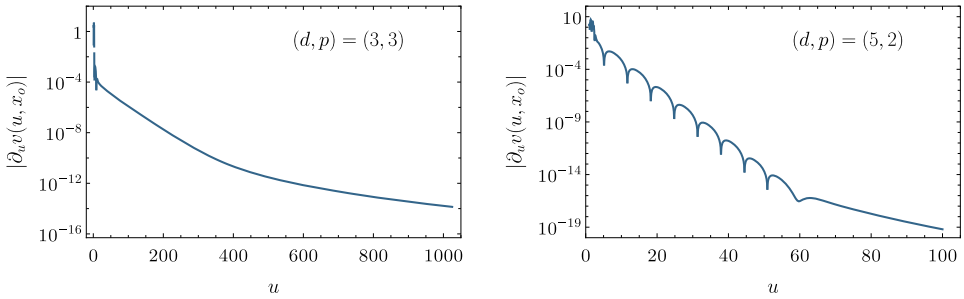

Figure A2. Pointwise decay (at a sample interior point $x_o=5/9$) of the linear perturbation of f_0 as governed by equation (23) for $(d,p)=(3,3)$ and $(d,p)=(5,2)$ for sample compactly supported initial data with the unstable mode removed. Numerical solution uses $N=1024$ Chebyshev polynomials, cf Fig. 3.

and performing diagonalization

$$\mathbf{D}^{-1}\mathbf{L}_n=\mathbf{P}\Lambda\mathbf{P}^{-1},\quad \Lambda=\mathrm{diag}\,(\Lambda_1,\ldots,\Lambda_N), \tag{27}$$

we solve the system (25) by exponentiation

$$\mathbf{v}(u)=\mathbf{P}\,\exp(\Lambda u)\,\mathbf{P}^{-1}\mathbf{v}(0), \tag{28}$$

where $\mathbf{v}(0)$ is a vector of initial data. As N grows, the eigenvalues Λ_i, $i=1,\ldots,N$ tend to the eigenvalues λ of (15), hence by increasing N we uncover more and more eigenvalues found in section 3 with the shooting method. This is illustrated in figure A1. The drawback of this method is the accumulation of spurious eigenvalues on the negative real axis which makes it hardly possible to extract the genuine eigenvalues lying on that axis (such as λ_2 for $d=3$).

Interestingly enough, using a large enough number of polynomials we were able (after removing the unstable mode from the initial data) to see in the evolution the polynomial tail whose exponent is in agreement with [12], cf figure A2.

ORCID iDs

Maciej Maliborski https://orcid.org/0000-0002-8621-9761

References

[1] Tao T 2006 *Nonlinear Dispersive Equations: Local and Global Analysis* (CBMS Regional Series in Mathematics) (Providence, RI: American Mathematical Society)
[2] Bizoń P, Chmaj T and Tabor Z 2004 On blowup for semilinear wave equations with a focusing nonlinearity *Nonlinearity* **17** 2187
[3] Donninger R and Schörkhuber B 2014 Stable blow up dynamics for energy supercritical wave equations *Trans. Am. Math. Soc.* **366** 2167
[4] Bizoń P, Maison D and Wasserman A 2007 Self-similar solutions of semilinear wave equations *Nonlinearity* **20** 2061
[5] Glogić I, Maliborski M and Schörkhuber B 2020 Threshold for blowup for the supercritical cubic wave equation *Nonlinearity* **33** 2143
[6] Glogić I and Schörkhuber B 2018 Codimension one stable blowup for the supercritical cubic wave equation (arXiv:1810.07681)
[7] Cazenave T 2006 *An Introduction to Semilinear Elliptic Equations* (Rio de Janeiro: Editora do IM-UFRJ)
[8] Rupflin M and Struwe M 2012 Supercritical elliptic equations *Adv. Nonlinear Stud.* **12** 877
[9] Duyckaerts T and Yang J 2019 Scattering to a stationary solution for the superquintic radial wave equation outside an obstacle (arXiv:1910.00811)
[10] Fowler R H 1930 The solutions of Emden's and similar differential equations *Mon. Not. Roy. Astron. Soc.* **91** 63
[11] Strauss W A and Tsutaya K 1997 Existence and blow up of small amplitude nonlinear waves with a negative potential *Discrete Cont. Dyn. Sys.* **3** 175
[12] Bizoń P, Chmaj T and Rostworowski A 2007 Anomalously small wave tails in higher dimensions *Phys. Rev.* D **76** 124035
[13] Gajic D and Warnick C 2019 A model problem for quasinormal ringdown on asymptotically flat or extremal black holes (arXiv:1910.08481)
[14] Bizoń P, Chmaj T and Rostworowski A 2008 Note on late-time tails of spherical nonlinear waves *Phys. Rev.* D **78** 024044
[15] Canuto C, Hussaini M Y, Quarteroni A and Zang T A 2007 *Spectral Methods, Evolution to Complex Geometries and Applications to Fluid Dynamics* (Berlin: Springer)